Thermal Stability and Molecular Interaction of Polyurethane Nanocomposites Prepared by *In Situ* Polymerization with Functionalized Multiwalled Carbon Nanotubes

R. N. Jana,[1] Jae Whan Cho[2]

[1]*Artificial Muscle Research Center, Konkuk University, Seoul 143-701, Korea*
[2]*Department of Textile Engineering, Konkuk University, Seoul 143-701, Korea*

Received 2 October 2007; accepted 25 November 2007
DOI 10.1002/app.27895
Published online 25 February 2008 in Wiley InterScience (www.interscience.wiley.com).

ABSTRACT: Polyurethane (PU) nanocomposites were prepared through conventional and *in situ* methods with multiwalled carbon nanotubes (MWNTs) functionalized with poly(ε-caprolactone). The thermal degradation and stability of PU–MWNT nanocomposites were investigated with nonisothermal thermogravimetry and were explained in terms of the interaction between MWNTs and PU molecules with Fourier transform infrared spectroscopy. The difference in thermal stability between the conventional and *in situ* nanocomposites was also compared. The thermal degradation of all the nanocomposite samples took place in two stages and followed a first-order reaction. The degradation temperature of the *in situ* nanocomposites was higher than that of the conventional nanocomposites with the same loading of MWNTs. The activation energy at 10% degradation and the half-life period were also higher in the *in situ* nanocomposites compared to the conventional nanocomposites. Such higher thermal stability of the *in situ* nanocomposites was ascribed to covalent bond formation between MWNTs and PU chains, which could result in better dispersion of MWNTs in the PU matrix for the *in situ* nanocomposites than for the conventional nanocomposites. © 2008 Wiley Periodicals, Inc. J Appl Polym Sci 108: 2857–2864, 2008

Key words: degradation; nanocomposites; polyurethanes; thermogravimetric analysis (TGA)

INTRODUCTION

The thermal degradation of polymer composites is important for predicting their suitability for end-use applications at high temperatures. For such purposes, thermogravimetric analysis is widely used with useful information such as the kinetics of decomposition and thermal lifetime.[1] The thermal stability and mode of decomposition of polymer composites are largely dependent on the chemical structure of the chain segments of the polymers and also on the nature of the interactions between the polymer and the reinforcing materials.[2] The mass loss during the degradation may be primarily due to chain scission of the base polymers leading to the elimination of degraded products, loss of the interaction between the polymer and filler and elimination of the phase-separated products, and elimination of low-molecular-weight components in the presence of physically bound moisture, a blowing agent, and unreacted raw materials.[2]

Polyurethane (PU) constitutes an important and versatile class of polymer materials that may find applications in areas requiring properties such as excellent flexibility, elasticity, and damping ability.[3] However, pure PU has some disadvantages, such as low mechanical strength, high water absorption, and poor thermal stability, that limit its high-temperature applications. As a method of improving the thermal stability of PU, the molecular structures, composed of hard and soft segments, can be tailored. Another way has also been used: making filler-reinforced composites with fillers such as carbon nanotubes (CNTs), which have very high thermal stability. However, the dispersion of CNTs in PU is usually poor because of low interfacial interaction with the matrix polymer, and thus the improvement of the desired property is not easily achieved in PU–CNT nanocomposites. As a result, many researchers have used functionalized CNTs in obtaining nanocomposites with improved mechanical and thermal properties.[4,5] Many examples have been reported in polymer matrices such as poly(methyl methacrylate), polyaniline, poly(vinyl alcohol), polystyrene, epoxy resin, and nylon 6.[6–12]

Correspondence to: J. W. Cho (jwcho@konkuk.ac.kr).
Contract grant sponsor: Korea Research Foundation; contract grant number: KRF-2004-005-B00046.
Contract grant sponsor: SRC/ERC program of MOST/Korea Science and Engineering Foundation; contract grant number: R11-2005-065.

Journal of Applied Polymer Science, Vol. 108, 2857–2864 (2008)

Covalent and noncovalent modification of CNTs has been employed to prepare polymer/CNT nanocomposites: direct incorporation of functionalized multiwalled carbon nanotubes (MWNTs) into polymer matrices (noncovalent attachment) and *in situ* polymerization at their surface (covalent attachment).[6,8] For the preparation of more thermally stable nanocomposites, the covalent attachment is considered to be more advantageous than the noncovalent attachment.[8] Many researchers have studied the thermal stability of polymer/CNT nanocomposites.[13–17] However, there are very few reports on the kinetics of degradation and degradation mechanism for PU/CNT nanocomposites.[18,19]

In this study, MWNTs grafted with poly(ε-caprolactone) diol (PCL) were employed to make PU nanocomposites because the PCL-based shape-memory PU was used as the matrix polymer. The PU–MWNT nanocomposites were prepared with two types of methods, conventional and *in situ*, and their thermal stability was compared. An evaluation of kinetic parameters such as the degradation temperatures, activation energy (ΔE), order of the reaction (n), half-life ($t_{1/2}$), and lifetime (t_f) was also made for the two types of PU/MWNT nanocomposites.

EXPERIMENTAL

Materials

MWNTs 10–20 nm in diameter and 20 μm long were purchased from Iljin Nanotech (Seoul, Korea). PCL (weight-average molecular weight = 3000; Solvay Co., Cheshire, UK), 4,4′-methylene bis(phenyl isocyanate) (MDI; Aldrich, St. Louis, MO), and 1,4-butane diol (BD; Junsei Chemicals, Tokyo, Japan) were used for this study.

Preparation of PU

The neat PU was synthesized with a two-step method from its monomers MDI, PCL, and BD in the molar ratio of 4 : 1 : 3 (Table I). Initially, the required quantities of MDI and PCL were added at a temperature of 80°C for 90 min to a four-necked cylindrical vessel equipped with a mechanical stirrer and a nitrogen flow. Then, BD as a chain extender was added slowly to the prepolymer at 110°C, and the reaction was allowed to continue for another 150 min. Finally, the synthesized PU was washed with water and dried overnight in an oven at 65°C *in vacuo*.

Preparation of conventional nanocomposites of PU and MWNTs

After the dissolution of neat PU in dimethylformamide, the temperature was raised to 80°C, the requisite quantity of MWNTs was added, and the mixing was continued for 12 h. The nanocomposites were dried overnight in an oven at 65°C *in vacuo* and were coded as C-0.5, C-1.5, and so forth; the numbers in the sample codes denote the weight percentage of MWNTs in the composites.

Preparation of *in situ* nanocomposites of PU and MWNTs

The carboxylated MWNTs were prepared by the treatment of MWNTs in a mixture of HNO_3 and H_2SO_4 (1/3 v/v) at 90–130°C for 120 min. The carboxylated MWNTs were reacted with thionyl chloride ($SOCl_2$) to get acyl chloride functionalized multiwalled carbon nanotubes (f-MWNTs). Then, f-MWNTs were reacted with a required quantity of PCL (Table I) at 65°C for 24 h to get PCL-*g*-MWNTs. The reaction procedure for PCL-*g*-MWNTs is shown in Figure 1.

With the same composition used for conventional composites, the PU prepolymer was synthesized by the reaction of MDI with PCL-*g*-MWNTs at 80°C for 90 min. Then, BD was added slowly to the prepolymer at 110°C, and the reaction was allowed for another 150 min. After the addition of about 100 mL of dimethylformamide, the temperature was reduced to 80°C, and the mixing was continued for another 12 h. Finally, the PU composites were washed with

TABLE I
Compositions of the PU/MWNTs Nanocomposites

Composite	MDI (mol %)	PCL (mol %)	BD (mol %)	MWNTs (wt %)	f-MWNTs (wt %)
PU	4	1	3	0	0
C-0.5	4	1	3	0.5	0
C-1.5	4	1	3	1.5	0
C-3.5	4	1	3	3.5	0
C-6.5	4	1	3	6.5	0
I-0.5	4	1	3	0	0.5
I-1.5	4	1	3	0	1.5
I-3.5	4	1	3	0	3.5
I-6.5	4	1	3	0	6.5

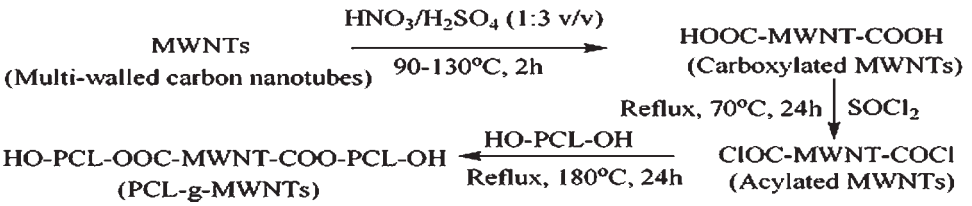

Figure 1 Reaction procedure for the preparation of PCL-*g*-MWNTs.

water and dried overnight in an oven at 65°C *in vacuo*, and they were coded I-0.5, I-1.5, and so forth; the numbers in the sample codes denote the weight percentage of f-MWNTs in the composites, as presented in Table I. The possible reaction procedure for the *in situ* nanocomposites is shown in Figure 2.

Measurements

Fourier transform infrared (FTIR) spectroscopy

FTIR spectroscopy measurements were performed with a Jasco FTIR 300E (Jasco Inc., Easton, MD) with an attenuated total reflectance method.

Thermogravimetric analysis

Thermogravimetry (TG) and derivative thermogravimetry (DTG) analysis of the nanocomposites and pure components were carried out in a thermogravimetric analyzer (TGA Q2050, TA Instruments, New Castle, DE) equipped with a computer data analyzer. The measurements were performed from room temperature to 600°C, except for MWNTs, in a nitrogen atmosphere at a flow rate of 50 mL/min and heating rate of 10°C/min. For each sample, three tests were performed at the same heating rate and in the same temperature range.

Determination of ΔE by the Freeman–Carroll method

ΔE for 10% decomposition of the composites and the order of the degradation reaction were determined with the standard kinetic equation by the Freeman–Carroll method:[20,21]

$$-dw/dt = Ae^{-\Delta E/RT}w^n \quad (1)$$

where dw/dt is the rate of the degradation reaction (mg/s), A is the pre-exponential factor (s^{-1}), ΔE is the activation energy (J/mol), R is the molar gas constant (8.314 J/mol/K), T is the absolute temperature (K), and w is the active weight at a particular time (mg). By taking the logarithm of eq. (1) and differentiating it, we derived the following equation:

$$\frac{d\ln(-dw/dt)}{d\ln w} = (-\Delta E/R)\frac{d(1/T)}{d\ln w} + n \quad (2)$$

From eq. (2), the values of ΔE and n were calculated.

Determination of $t_{1/2}$ and t_f by the Flynn–Wall method

$t_{1/2}$ was defined as the lifespan of the material when the weight of the sample became half of its initial value. t_f of the polymer to failure was defined as the value of w when it became 1/20 of its initial value (i.e., 5% remaining).[22]

$t_{1/2}$ and t_f of the composites were estimated at 200°C with the Flynn–Wall method.[23] Assuming that the rate constant of the decomposition reaction (k) is independent of temperature and that the degradation reaction is to have first-order reaction kinetics, $t_{1/2}$ and t_f can be obtained as follows:

$$t_{1/2} = \frac{\ln 2}{k} = \frac{0.693}{k} \quad (3)$$

$$t_f = \frac{\ln 20}{k} = \frac{2.996}{k} \quad (4)$$

where k denotes $Ae^{-\Delta E/RT}$ and n equals unity.

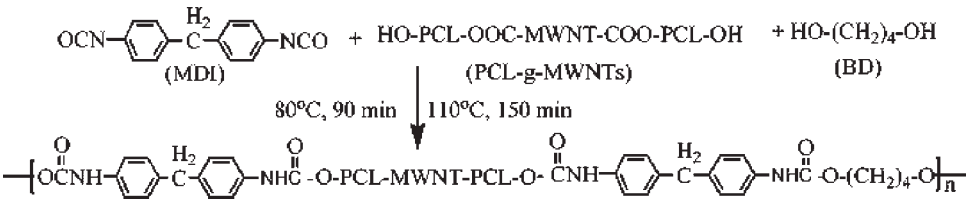

Figure 2 Possible reaction procedure of the nanocomposites prepared by the *in situ* method.

Scanning electron microscopy (SEM) and transmission electron microscopy (TEM) observations

The morphology of the cryogenically fractured surface of pure PU and the nanocomposites was observed with a scanning electron microscope (S-4200, Hitachi, Tokyo, Japan). The fractured surface was sputter-coated with gold to facilitate scanning under SEM at a 0° tilt angle. For MWNTs, the powder sample was sputter-coated with gold.

The morphological analysis was also carried out with TEM. Samples for TEM were prepared by the dispersion of the sample in ether and subsequent placement of a drop of the suspension on one side of the transparent polymer-coated 200-mesh copper grid. TEM images were taken with a Zeiss LIBRA-120 (Tokyo, Japan), the energy-filtering TEM being combined with state-of-the-art electron optics with unique Koehler illumination.

RESULTS AND DISCUSSION

FTIR analysis

Figure 3 shows FTIR spectra of unmodified MWNTs, and a peak with very low intensity at 1637 cm^{-1} due to C=O stretching can be seen, indicating the presence of a small number of carboxylic groups in MWNTs as impurities.[4] After oxidation with the mixture of acids, the C=O stretching is shifted to 1695 and 1644 cm^{-1}. These peaks are assigned to free carbonyl groups and hydrogen-bonded carbonyl groups of the MWNTs, respectively.[15] Acylation of carboxylic groups leads to the formation of a carbonyl peak at 1722 cm^{-1} with one new peak at 829 cm^{-1}. The new peak may be due to C—Cl bond formation. After the reaction with PCL along with

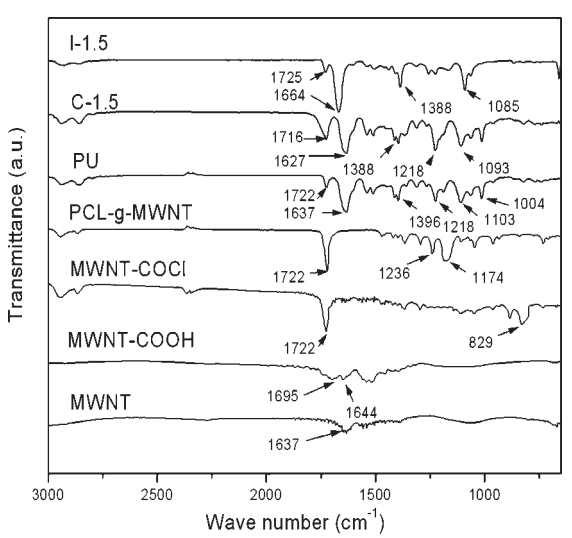

Figure 3 FTIR spectra of PU, the MWNTs, and samples C-0.5 and I-0.5.

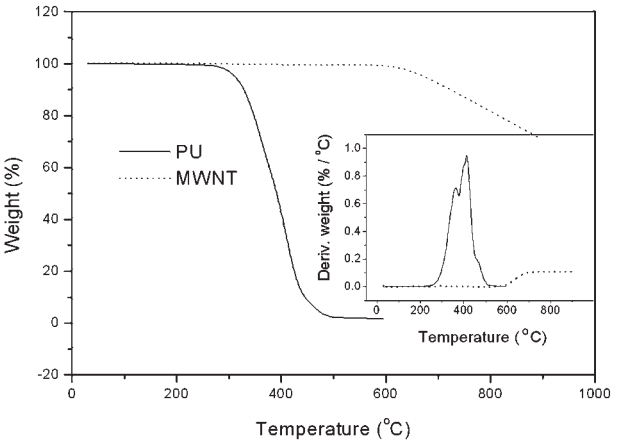

Figure 4 TG and DTG of the MWNTs and PU.

the carbonyl peak, the peaks at 1236 and 1174 cm^{-1} appear, and they are due to C—O stretching coming from the reaction between the —COCl group of the f-MWNT and the —OH group of PCL. The neat PU shows a very weak peak at 1722 cm^{-1} corresponding to the free carbonyl group, a sharp peak at 1637 cm^{-1} for the carbonyl group of the urethane linkage, a peak at 1396 cm^{-1} for C—H scissoring and bending coming from BD, and peaks at 1218, 1103 and 1004 $cm^{-1}$for C—O stretching of the backbone chain. In the case of the conventional nanocomposites (e.g., C-1.5), no new peak is found; all the peaks have come from the raw MWNTs and neat PU, and this implies a poor interaction between the constituents. Here the interaction between the PU chain and the MWNTs is mainly due to the physical entanglement. For *in situ* nanocomposites (e.g., I-1.5), the peaks at 1664, 1388, and 1085 cm^{-1} correspond to the carbonyl of the urethane linkage, C—H scissoring and bending from BD, and C—O stretching of the backbone chain coming from the reaction with diisocyanate and PCL-*g*-MWNTs, respectively. The MWNTs remain inside as a part of the PU chain (Fig. 2). As a result, there is a strong interaction between PU and MWNTs in the form of covalent bond formation.

Effect of MWNTs on thermal degradation

Figure 4 shows TG and DTG curves of MWNTs and PU. The initial degradation temperature (T_i) values corresponding to 1% decomposition for neat PU and MWNTs are 273 and 604°C, respectively. The first maximum decomposition temperature (T_{1max}) and second maximum decomposition temperature (T_{2max}) for PU are 362 and 412°C, respectively, indicating two-stage degradation of PU. The initial degradation of PU is due to the dissociation of the urethane linkage to form isocyanate and alcohol, and the second stage of degradation is the dissociation of isocyanate

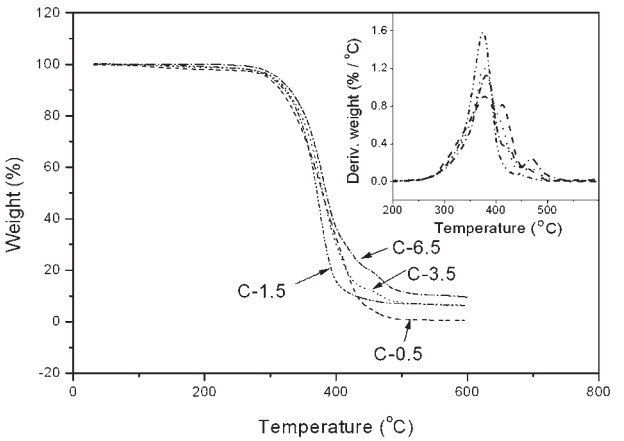

Figure 5 TG and DTG of the conventional nanocomposites.

and alcohol to a primary or secondary amine, olefin, and carbon dioxide.[24,25] However, MWNTs show very slow single-stage degradation at 731°C, which is responsible for the degradation of the impurities present in MWNTs, such as amorphous carbon and metal oxides, and the breakdown of their length at the defect sites.

TG and DTG curves for the conventional nanocomposites are shown in Figure 5. As the weight proportion of MWNTs in the composites increases from 0.5 to 6.5%, the T_i value decreases gradually from 216 to 185°C, as presented in Table II. These T_i values of conventional composites are lower than that of pure PU. This may be due to the presence of a small number of carboxylic groups as impurities remaining on the MWNTs as the carbon atom of MWNTs attached to the carboxylic group is sp^3-hybridized and therefore more susceptible to thermal degradation. However, all the conventional nanocomposites undergo the first stage of degradation within the temperature range of 374–376°C. As the values for temperature at which 50% of the material has been degraded (T_{50}) and T_{1max} are close enough, it seems that during the first stage of degradation, which corresponds to the dissociation of mainly the PU chains into diisocyanate and diol, almost 50% loss occurs. Moreover, T_{2max} and T_f (the temperature of the finish) increase with the increase in the weight percentage of MWNTs in the composites. This may be due to the effect of MWNTs as a thermal barrier against the further dissociation of diisocyanate and diol, which are formed during the first stage of degradation of PU/MWNT composites.

TABLE II
Degradation Temperatures of the Pure Components and Nanocomposites

Sample	T_i (°C)	T_{1max} (°C)	T_{2max} (°C)	T_{50} (°C)	T_f (°C)
PU	273	362	412	391	510
MWNT	604	731	—	—	—
C-0.5	216	376	412	378	474
C-1.5	198	376	464	377	493
C-3.5	189	375	469	375	506
C-6.5	185	374	472	371	509
I-0.5	245	412	463	399	486
I-1.5	240	415	466	408	513
I-3.5	234	421	471	409	516
I-6.5	227	425	475	410	520

TG and DTG curves for the *in situ* composites are shown in Figure 6, and the degradation temperatures are tabulated in Table II. There is also a decreasing trend in the T_i values with the increasing weight percentage of MWNTs in the composites as observed in the case of conventional nanocomposites. The increased proportion of carboxylic groups coming from the acid-treated MWNTs leads to an early stage of thermal degradation. However, the T_i values of *in situ* composites are higher than those of conventional composites because of better interaction between MWNTs and PU chains. However, T_{1max}, T_{2max}, T_{50}, and T_f for the composites increase gradually with the weight percentage of MWNTs in the composites. This may be due to more polymer–filler interaction in the composites as well as the properties of MWNTs as a barrier, which delays the degradation of the composites. Moreover, all the degradation temperatures for the *in situ* nanocomposites are always higher than those for the conventional nanocomposites with the same loading of MWNTs. This implies that in the case of the *in situ* nanocomposites, the degradation starts at a later stage and persists for a longer time. Thus, the *in situ* nanocomposites are more thermally stable than the conventional nanocomposites. It is also clear from the relation between the extent of degradation and temperature, as shown in Figure 7. For the *in situ* nanocomposites, the extent of degradation is lower than that for the conventional nanocomposites. This may be due to the formation of stable chemical

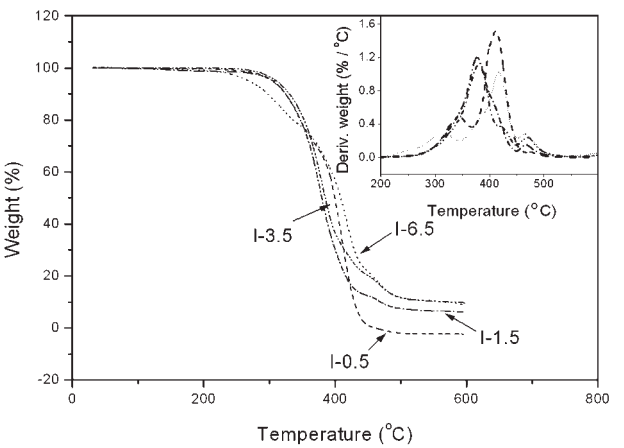

Figure 6 TG and DTG of the *in situ* nanocomposites.

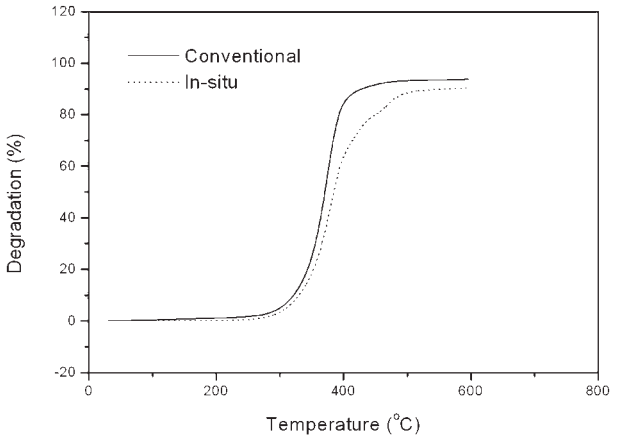

Figure 7 Extent of degradation with temperature for the conventional and *in situ* nanocomposites with 6.5 wt % MWNTs.

bonds between the constituents, as confirmed by the previous FTIR results.

Effect of MWNTs on ΔE of thermal degradation

The ΔE values and order of the degradation reaction for the base materials and the composites are summarized in Table III. The ΔE values for PU and MWNTs were found to be 163.6 and 312.6 kJ/mol, respectively. This indicates that in the initial stage of degradation, MWNTs need higher ΔE for the degradation process than that of PU because of the inherently higher thermal stability of MWNTs. The values of n for PU and MWNTs were calculated to be 1.05 and 0.98, respectively. This indicates that the degradation reaction is a first-order reaction.

ΔE of the conventional nanocomposites is lower than that of the neat PU. Because the unmodified MWNTs were used in conventional nanocomposites, there may be very low reinforcement with the PU chain, and the interaction is mainly from physical entanglement. MWNTs can also enter into the PU molecular chains, thereby increasing the intermolecular distance or rather decreasing the intermolecular force of attraction. Consequently, the low-molecular-weight chain may be more easily degraded and eliminated from the composites. Therefore, there is the reduced ΔE value for the composites, which is also in agreement with the lower T_i of the composites. However, there is an increasing trend in ΔE with the weight percentage of MWNTs in the composites. The increase in ΔE with the increase in the weight percentage of MWNTs is due to the higher reinforcement. n is also unity for the conventional nanocomposites.

ΔE for the *in situ* nanocomposites is always higher than that for the neat PU or conventional nanocomposites, as shown in Table III. The I-6.5 nanocomposite has the maximum ΔE value of 210.9 kJ/mol among all the composites. This is due to the formation of covalent bonds between the MWNTs and PU chains. Moreover, n has a value very close to unity. It well corresponds to the earlier assumption of the first-order reaction used in obtaining ΔE values of the thermal degradation of the samples.

Effect of MWNTs on $t_{1/2}$ and t_f

The values of $t_{1/2}$, determined at 200°C for PU and MWNTs, were found to be 66.0 and 873.2 h, respectively. Similarly, the values of t_f for PU and MWNTs at the same temperature are 285.5 and 3775.0 h, as presented in Table III. For the conventional nanocomposites, the $t_{1/2}$ and t_f values are lower than those of neat PU. In the case of *in situ* nanocomposites, their values are lower at a loading of MWNTs lower than 1.5 wt %, but at a loading higher than 1.5 wt %, they are higher than those for neat PU. Moreover, *in situ* nanocomposites have higher $t_{1/2}$ and t_f values than those for the conventional nanocomposites with the same loading of MWNTs. The I-6.5 nanocomposite has the maximum $t_{1/2}$ value of 92.7 h and t_f value of 400.6 h. This is ascribed to better bonding between MWNTs and PU chains, as explained earlier.

Effect of MWNTs on the morphology of the nanocomposites

Figure 8(a) shows SEM photographs of neat PU. The cryogenically fractured surface is almost smooth; however, the neat MWNTs show a random arrangement of the nanotubes, with a few agglomerations in some places, as shown in Figure 8(b). Figure 8(c) shows the SEM pictures of the conventional nanocomposites containing 0.5 wt % MWNTs, and a few aggregated structures of MWNTs can be seen in some places. This indicates that the dispersion of MWNTs is not good because of low interfacial

TABLE III
ΔE, n, $t_{1/2}$, and t_f Values of the Pure Components and the Nanocomposites

Sample	ΔE (kJ/mol)	n	$t_{1/2}$ (h)	t_f (h)
PU	163.6	1.05	66.0	285.5
MWNT	312.6	0.98	873.2	3775.0
C-0.5	126.5	0.98	10.5	45.4
C-1.5	131.7	0.98	17.2	74.2
C-3.5	141.0	0.99	22.7	98.2
C-6.5	157.5	1.02	23.6	102.1
I-0.5	168.1	0.98	49.0	211.9
I-1.5	177.9	0.99	63.1	272.9
I-3.5	190.4	1.12	75.4	325.8
I-6.5	210.9	1.02	92.7	400.6

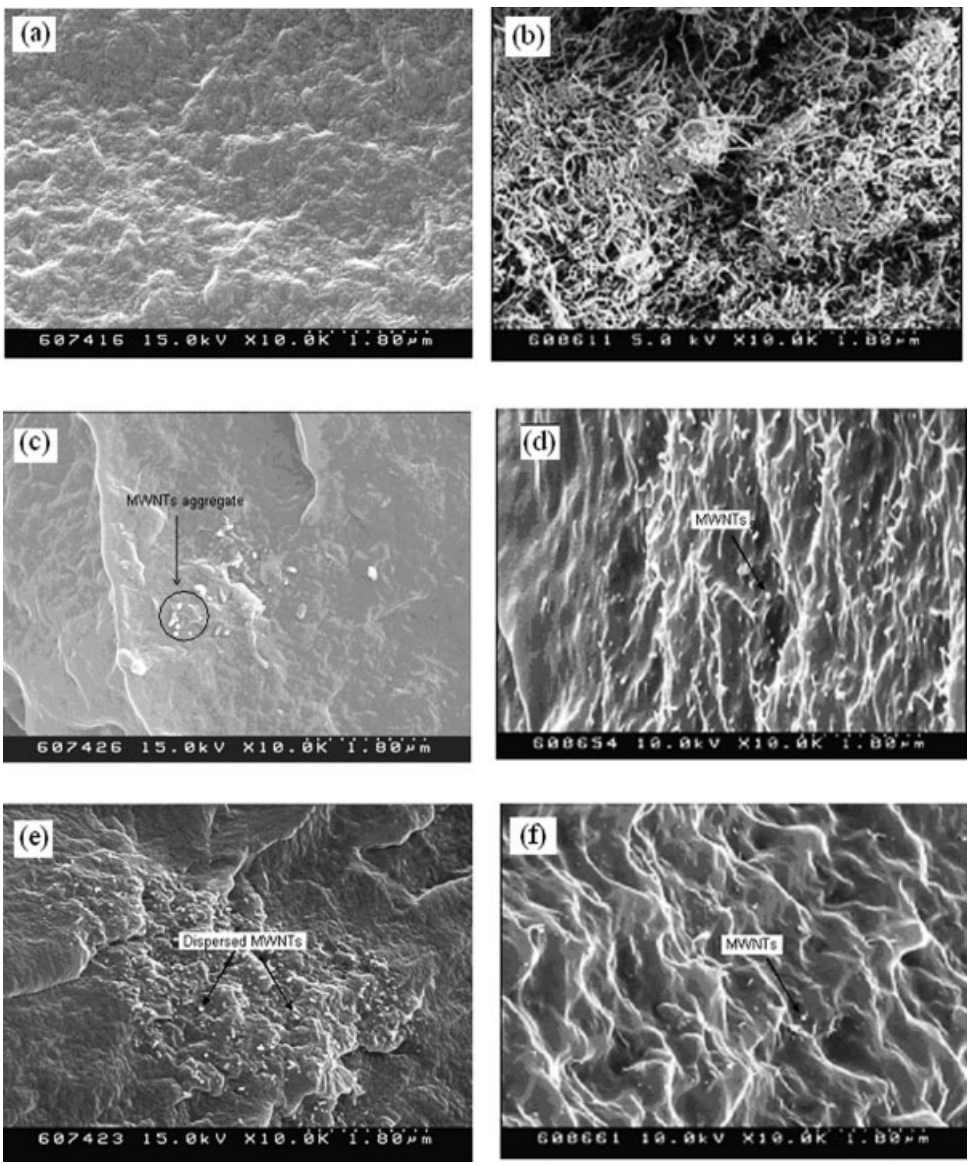

Figure 8 SEM photographs at 10,000× of (a) PU, (b) the MWNTs, (c) C-0.5, (d) C-6.5, (e) I-0.5, and (f) I-6.5.

interactions between the MWNTs and PU. A similar trend has also been observed at a high loading of MWNTs, as in Figure 8(d). Figure 8(e) shows the SEM photographs for the I-0.5 nanocomposite. The I-0.5 sample with a low proportion of MWNTs has a better dispersion of MWNTs than the C-0.5 nanocomposite because of the good interaction in the form of covalent bond formation. Figure 8(f) shows the SEM photographs of the *in situ* nanocomposites with 6.5 wt % MWNTs. It also shows a smaller domain size of the dispersed MWNTs. Moreover, the fractured surface of the I-6.5 sample shows a rib- or channel-like structure. This indicates that the applied stress can be transferred uniformly through the MWNTs to the polymer matrix. This may be due to the formation of chemical bonds between the MWNTs and the PU chain. The nanocomposites having better MWNT dispersion result in higher thermal stability.

Figure 9 shows the TEM photographs of C-0.5, C-3.5, I-0.5, and I-3.5 nanocomposites. Figure 9(a,c) shows that the MWNTs remain intact; there is no appreciable breakdown of their length, and they remain as the aggregated structure. However, in Figure 9(b,d), it is clear that the MWNTs are dispersed and distributed throughout the matrix almost uniformly. The TEM results also indicate a better dispersion of MWNTs in the *in situ* nanocomposites than in the conventional nanocomposites.

CONCLUSIONS

The PU, MWNTs, and nanocomposites have an almost first-order reaction in thermal degradation.

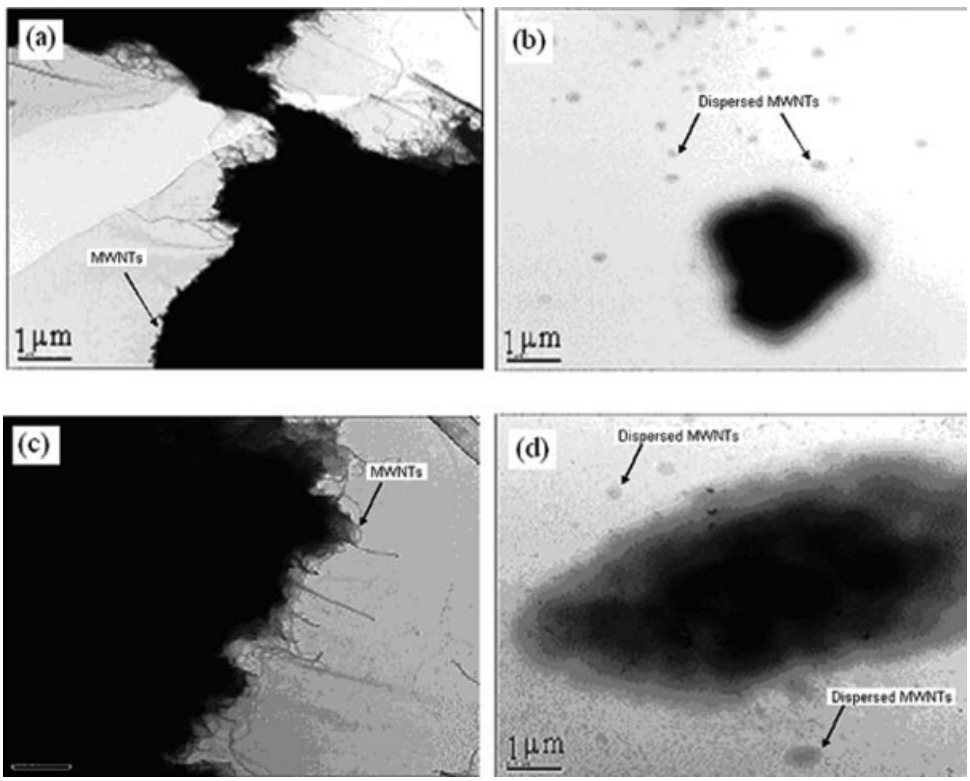

Figure 9 TEM photographs of (a) C-0.5, (b) I-0.5, (c) C-3.5, and (d) I-3.5.

T_i shifts toward a lower temperature for both nanocomposites with a higher proportion of MWNTs. The *in situ* nanocomposite with 6.5 wt % MWNTs shows the highest thermal stability and the maximum $t_{1/2}$ and t_f values. ΔE of the degradation reaction is always higher for *in situ* nanocomposites than for conventional nanocomposites with the same loading of MWNTs. The higher thermal stability of the *in situ* nanocomposites is due to the formation of covalent bonds between the MWNTs and PU chain.

References

1. Chang, W. L. J Appl Polym Sci 1994, 53, 1759.
2. Rosenberg, Y.; Siegmann, A.; Narkis, M.; Shkolnik, S. J Appl Polym Sci 1992, 45, 783.
3. Xiong, J.; Liu, Y.; Yang, X.; Wang, X. Polym Degrad Stab 2004, 86, 549.
4. Sahoo, N. G.; Jung, Y. C.; Yoo, H. J.; Cho, J. W. Macromol Chem Phys 2006, 207, 1773.
5. Gao, J.; Itkis, M. E.; Yu, A.; Bekyarova, E.; Zhao, B.; Haddon, R. C. J Am Chem Soc 2005, 127, 3847.
6. Hwang, G. L.; Shieh, Y. T.; Hwang, K. C. Adv Funct Mater 2004, 14, 487.
7. Baibarac, M.; Baltog, I.; Lefrant, S.; Mevellec, J. Y.; Chauvet, O. Chem Mater 2003, 15, 4149.
8. Chen, J.; Liu, H.; Weimer, W. A.; Halls, M. D.; Waldeck, D. H.; Walker, G. C. J Am Chem Soc 2002, 124, 9034.
9. Lin, Y.; Zhou, B.; Shiral Fernando, K. A.; Liu, P.; Allard, L. F.; Sun, Y. P. Macromolecules 2003, 36, 7199.
10. Hill, D. E.; Lin, Y.; Rao, A. M.; Allard, L. F.; Sun, Y. P. Macromolecules 2002, 35, 9466.
11. Eitan, A.; Jiang, K.; Dukes, D.; Andrews, R.; Schadler, L. S. Chem Mater 2003, 15, 3198.
12. Liu, T.; Phang, I. Y.; Shen, L.; Chow, S. Y.; Zhang, W. D. Macromolecules 2004, 37, 7214.
13. Wei, H. F.; Hsiue, G. H.; Liu, C. Y. Compos Sci Technol 2007, 67, 1018.
14. Chen, G. X.; Kim, H. S.; Park, B. H.; Yoon, J. S. Polymer 2006, 47, 4760.
15. Kang, M.; Myung, S. J.; Jin, H. J. Polymer 2006, 47, 3961.
16. Goh, H. W.; Goh, S. H.; Xu, G. Q.; Pramod, K. P.; Zhang, W. D. Chem Phys Lett 2003, 379, 236.
17. Fenga, W.; Bai, X. D.; Lian, Y. Q.; Liang, J.; Wang, X. G.; Yoshino, K. Carbon 2003, 41, 1551.
18. Mondal, S.; Hu, J. L. J Elast Plast 2006, 38, 261.
19. Xiong, J.; Zheng, Z.; Qin, X.; Li, M.; Li, H.; Wang, X. Carbon 2006, 44, 2701.
20. Encyclopedia of Polymer Science and Technology; Reich, R. L.; Levi, D. W.; Bikales, N. M., Eds.; Wiley-Interscience: New York, 1971; Vol. 14, p 7.
21. Freeman, E. S.; Carroll, B. J Phys Chem 1958, 62, 394.
22. Li, X. G.; Huang, M. R.; Guan, G. H.; Sun, T. Polym Int 1998, 46, 289.
23. Flynn, J. H.; Wall, L. A. Polym Lett 1966, 4, 323.
24. Bilbao, R.; Mastral, J. F.; Ceamanos, J.; Aldea, M. E. J Anal Appl Pyrolysis 1996, 37, 69.
25. Herrera, M.; Matuschek, G.; Kettrup, A. Polym Degrad Stab 2002, 78, 323.